

## Inelastic behavior of systems with flexible base

Luciano R. Fernández-Sola\* and Juan E. Huerta-Écatl

Departamento de Materiales, Universidad Autónoma Metropolitana-Azcapotzalco, San Pablo #180 Z.C. 02200, Mexico

(Received February 28, 2017, Revised February 6, 2018, Accepted March 15, 2018)

**Abstract.** This study explores the inelastic behavior of systems with flexible base. The use of a single degree of freedom system (ESDOF) with equivalent ductility to represent the response of flexible base systems is discussed. Two different equations to compute equivalent ductility are proposed, one which includes the contribution of rigid body components, and other based on the overstrength of the structure. In order to assess the accuracy of ESDOF approach with the proposed equations, the behavior of a 10-story regular building with reinforced concrete (RC) moment resisting frames is studied. Local and global ductility capacity and demands are used to study the modifications introduced by base flexibility. Three soil types are considered with shear wave velocities of 70, 100 and 250 m/s. Soil-foundation stiffness is included with a set of springs on the base (impedance functions). Capacity curves of the building are computed with pushover analysis. In addition, non linear time history analysis are used to assess the ductility demands. Results show that ductility capacity of the soil-structure system including rigid body components is reduced. Base flexibility does not modify neither yield and maximum base shear. Equivalent ductility estimated with the proposed equations fits better the results of the numerical model than the one considering elastoplastic behavior. Modification of beams ductility demand due to base flexibility are not constant within the structure. Some elements experience reduced ductility demands while other elements experience increments when flexible base is considered. Soil structure interaction produces changes in the relation between yield strength reduction factor and structure ductility demand. These changes are dependent on the spectral shape and the period of the system with fixed and flexible base.

**Keywords:** dynamic soil structure interaction; inelastic behavior; ductility demands; equivalent single degree of freedom model; RC buildings

### 1. Introduction

Structural design of buildings under seismic excitations considers that structures will undergo into inelastic behavior, which provides additional capacity and energy dissipation. In order to achieve a stable performance under inelastic behavior, the ductility and capacity of the building must be studied. Modern codes include design procedures based on the force reductions associated with non-linearity on the structure. In these procedures, specific collapse mechanisms are assumed (e.g., weak beam-strong column). When the base of the structure is considered fixed, the whole displacement is associated with structural deformations. Under these considerations, the ductility of the structure is defined directly by the ratio of maximum and yield displacements.

In some cases, the structures supporting soil is not stiff enough to produce a fixed base condition and soil properties become critical to structure performance. The interaction between soil and foundation can modify the dynamic properties of the soil-structure system, the characteristics of the excitation and soil behavior. The effects which arise from soil-foundation joint performance are defined as Dynamic Soil Structure Interaction (DSSI). The variation of structural period (lengthening) and damping produced by

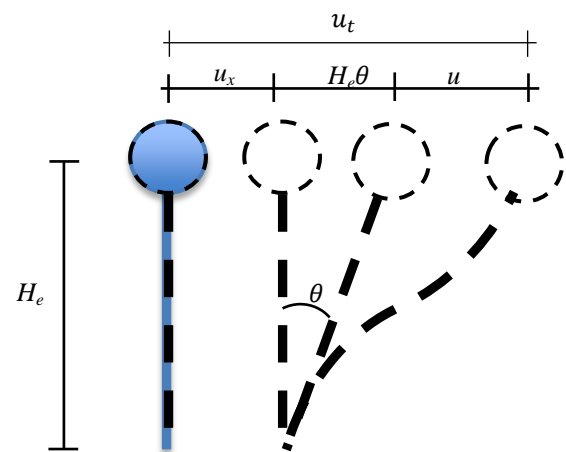


Fig. 1 Displacement components of the structure with flexible base

system flexibilization are the most recognized (Wolf 1985). These variations produce a modification on the spectral acceleration which the structure will experience. Procedures included on building codes (MCBC 2004, ASCE-7 2010, NZS, 3101-1 2006, NBCC 2015) use the base shear variation associated with spectral acceleration shift to compute changes of remaining response quantities (e.g., displacements, element forces, etc). Soil-foundation flexibility can be represented by its stiffness in different directions (e.g., horizontal= $K_x$  and rotational= $K_r$ ). Even

\*Corresponding author, Professor  
E-mail: [lrf@azc.uam.mx](mailto:lrf@azc.uam.mx)

though these DSSI implications are the most used, other effects of base flexibility could be also important.

Relative displacements between the structure supports and ground are produced due to base flexibility. Total displacement of the soil-structure system includes two principal components, one introduced by structural deformation ( $u$ ) and other due to a rigid body behavior ( $u_x$  and  $\theta$ ) as shown on Fig. 1. Since total displacement is not directly associated with structure deformation, the relation between ductility, defined as before, and inelastic deformation of the structure changes, as shown on the following.

Inelastic behavior of structures with flexible base has been previously studied. Some studies use an equivalent system with a single degree of freedom (ESDOF) in order to represent the system with flexible base (Rosenblueth and Resendiz 1988, Avilés and Pérez-Rocha 2005, Ghannad and Ahmadnia 2006, Eser *et al.* 2011). The equivalent properties (fundamental period, damping ratio and ductility) of the ESDOF system are set to reproduce the inelastic response of the system with flexible base.

This work explores the inelastic behavior of systems with flexible base. The influence of post yield stiffness is discussed. Two different equations to compute equivalent ductility considering post yield stiffness are proposed. In order to evaluate the equations, inelastic behavior of a 10 story regular building with RC frames with fixed and flexible base are studied. Non linear static analysis (pushover) is performed in order to establish the inelastic capacity of the structures.

In addition, the non linear dynamic behavior of the buildings are analyzed, under the same assumptions than non linear static analysis. The modifications of the hysteretic loops of the whole building and local and global ductility demands are studied. The variation of ductility demands over the height are discussed.

## 2. Equivalent ductility on flexible base systems

Ductility of the ESDOF system ( $\tilde{\mu}$ ) can be expressed as a function of the equivalent period ( $\tilde{T}$ ) and the fundamental period and ductility of the system with fixed base ( $T$  and  $\mu$ ) with Eq. (1) for an elastoplastic system.

$$\tilde{\mu} = \left(\frac{T}{\tilde{T}}\right)^2 (\mu - 1) + 1 \tag{1}$$

Equivalent ductility ( $\tilde{\mu}$ ) must be used to compute the strength reduction factor ( $R_\mu$ ) in order to reproduce the behavior of the system with flexible base. This equivalent ductility always yields to smaller values than the ductility of the fixed base system ( $\tilde{\mu} \leq \mu$ ), since  $\tilde{T}$  is always larger or equal than  $T$ . It does not mean that base flexibility produces a reduction on the inelastic capacity of the system, a concept that is commonly misunderstood. Ductility of the ESDOF system must be modified due to a change on the ratio of  $R_\mu$  and  $\mu$  produced by base flexibility. If elastic seismic forces are reduced by  $R_\mu$  computed with the target ductility of the system with fixed base, then ductility demands on the structure with flexible base may be larger

than the target ductility, as shown by Jarenpasert *et al.* (2013). In order to illustrate this effect, consider an inelastic ESDOF system. For structures with larger fundamental period than the dominant period of the excitation, maximum displacements of the elastic and inelastic systems are equal and the strength reduction factor  $\llbracket(R)_\mu$  becomes equal to ductility ( $\mu$ ) (Chopra 2012).

As shown on Fig. 1, total displacement of the system with flexible base ( $u_t$ ) considers the displacements due to rigid body behavior ( $u_{RB}=u_x+H_e\theta$ ) and deformation of the structure ( $u$ ). Ductility of the ESDOF system ( $\tilde{\mu}$ ) is defined by Eq. (2). In the following deduction, superscript  $y$  stands for displacements at structures yield, while superscript  $u$  stands for the maximum displacement.

$$\tilde{\mu} = \frac{u_t^u}{u_t^y} \tag{2}$$

where:

- $u_t^u = u_{RB}^u + u^u$  maximum displacement of the soil-structure system
- $u_{RB}^u$  maximum displacement due to rigid body
- $u^u$  maximum deformation of the structure
- $u_t^y = u_{RB}^y + u^y$  yield displacement of the soil-structure system
- $u_{RB}^y$  rigid body displacement at yield displacement
- $u^y$  deformation of the structure at yield displacement

For a target ductility of the ESDOF system of  $\tilde{\mu} = 2$ , the corresponding strength reduction factor will be  $R_\mu = V_0/V_y = 2$  (Fig. 2(a)). Let  $u_t^y$  be 2 then, maximum total displacement

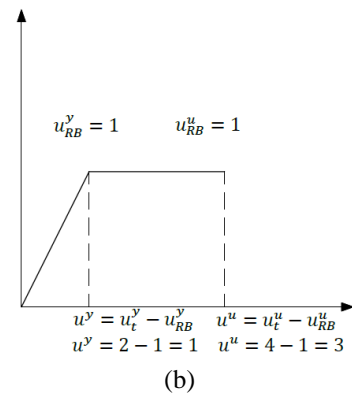
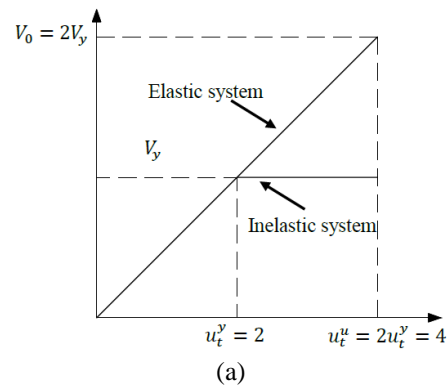


Fig. 2 Inelastic behavior of the ESDOF system and the structure

becomes  $u_t^u = \tilde{\mu}u_t^y = 4$ . The displacements due to rigid body behavior can be estimated as the ratio of base shear and foundation horizontal stiffness ( $u_x = V_0/K_x$ ) and the ratio of the overturn moment and the foundation rocking stiffness ( $\phi = M_0/K_r$ ). Since the system is elastoplastic, base shear and overturn moment remains constant on the inelastic behavior ( $V_y = V_u$  and  $M_y = M_u = V_y H_e$ ). Considering that the soil-foundation system remains elastic, implies that  $K_x$  and  $K_r$  are not modified, the displacement produced by rigid body behavior of the structure at yield and maximum displacement must be the same ( $u_{RB}^y = u_{RB}^u$ ). If it is supposed that  $u_{RB}^y = u_{RB}^u = 1$ , then the deformation of the structure at yield and maximum displacement become  $u^y = 1$  and  $u^u = 3$  (Fig. 2(b)). With these values, the structure must develop a ductility of 3 (Eq. (3))

$$\mu = \frac{u^u}{u^y} = 3 \quad (3)$$

which is larger than the target ductility of the EDOF system. So, if the desired target ductility demand in the structure is  $\mu = 2$ , a reduced  $R_\mu$  value computed with  $\tilde{\mu}$  in stead of  $\mu$  must be considered. The need of reduced  $R_\mu$  values for flexible base systems, in order to keep a target has been previously described and identified (Jarernprasert *et al.* 2013, Halabian and Erfani 2013, Aydemir and Ekiz 2013).

This procedure considers that ESDOF behaves as a perfect elastoplastic system, with no post yield stiffness. However, laterally redundant systems experiment a progressive yield, that must be modeled as a bilinear system with post yield stiffness. In the following section, the contribution of post yield stiffness is discussed.

ESDOF approach is very useful and yields to good results in a lot of cases (Avilés and Pérez-Rocha 2005, 2011). Since just one degree of freedom is used, this procedure considers that modifications introduced by base flexibility in all structural responses along the structure will be linearly equivalent. However, previous studies have shown that the representation of a system with multiple degrees of freedom and flexible base with an ESDOF system may not be accurate in some cases.

Barcena and Esteva (2007) studied the ductility demands on multistory systems with flexible base. They found that the modification of the ductility demands produced by DSSI are different along the structure height. This effect can not be represented by an ESDOF system. Ganjavi and Hao (2011) compared the modification on the global ductility demand of structures modeled with flexible base considering multiple degrees of freedom and with the ESDOF approach. Results prove that for very flexible structures, ductility demands with flexible base computed with the ESDOF approach are smaller than the ones computed with the multiple degrees of freedom systems. On the other hand, Fernández-Sola *et al.* (2014, 2015) studied the capacity curves of steel braced frames with flexible base. They concluded that in general, the inelastic capacity of the systems with fixed and flexible base are very similar.

Ghandil and Behnamfar (2017) studied the inelastic behavior of moment resistant frames buildings with flexible base. They analyzed the rotational ductility demands on beams and columns and found that variations on ductility

demands along structures height due to base flexibility are not constant, as well as Barcena and Esteva. The greater increments on story drift are concentrated on the lower stories.

### 3. Post yield stiffness on systems with flexible base

As shown above, the relation between  $R_\mu$  and  $\mu$  is controlled by the modification of contribution of rigid body components when the structure undergoes inelastic behavior. For systems with post yield stiffness, the displacement due to rigid body components does not remain constant for the plastic branch (Avilés and Pérez-Rocha 2011). In order to include this effect, the following procedure is proposed. If the system ductility is expressed in terms of rigid body displacement and deformation of the structure, it can be established that (Eq. (4))

$$u_{RB}^u + u^u = \tilde{\mu}(u_{RB}^y + u^y) \rightarrow u^u \left(1 + \frac{u_{RB}^u}{u^u}\right) = \tilde{\mu}u^y \left(1 + \frac{u_{RB}^y}{u^y}\right) \quad (4)$$

To compute the ductility in the structure ( $\mu$ ), it must be considered only the displacement produced by deformation of the structure. In consequence, the relation between the equivalent system ductility with flexible base ( $\tilde{\mu}$ ) and ductility in the structure ( $\mu$ ) can be defined as (Eq. (5))

$$\mu = \frac{u^u}{u^y} = \tilde{\mu} \frac{\left(1 + \frac{u_{RB}^y}{u^y}\right)}{\left(1 + \frac{u_{RB}^u}{u^u}\right)} \rightarrow \tilde{\mu} = \mu \frac{\left(1 + \frac{u_{RB}^u}{u^u}\right)}{\left(1 + \frac{u_{RB}^y}{u^y}\right)} \quad (5)$$

If the contribution of rigid body components to the total displacement remains constant for yield and maximum displacement, ductility on the structure is equal to the ductility on the system. If the contribution is modified, the ratio between  $\tilde{\mu}$  and  $\mu$  is not equal to 1, and values of  $\tilde{\mu}$  and  $\mu$  becomes different. Eq. (5) can be used if the contribution of each displacement component is known at yield and maximum displacement. However, for design purposes, the exactly contribution of the different displacement components is not known in advance. In order to establish a suitable design equation which takes into account the post yield stiffness, the overstrength factor of the structure can be used. Overstrength factor can be defined as the ratio of maximum base shear and yield base shear ( $\Omega = V_u/V_y$ ). Total yield displacement ( $u_t^y$ ) can be expressed in terms of yield base shear ( $V_y$ ), elastic stiffness of the structure ( $K$ ) and soil-foundation stiffness ( $K_x$  and  $K_r$ ) as (Eq. (6))

$$u_t^y = \frac{V_y}{K} + \frac{V_y}{K_x} + \frac{V_y(H_e)^2}{K_r} = V_y \left( \frac{1}{K} + \frac{1}{K_x} + \frac{(H_e)^2}{K_r} \right) \quad (6)$$

where:

$$\frac{V_y}{K} = u^y \quad \text{and} \quad \frac{V_y}{K_x} + \frac{V_y(H_e)^2}{K_r} = u_{RB}^y$$

In addition, total maximum displacement ( $u_t^u$ ) can be expressed in terms of yield base shear. Defining the

maximum base shear as  $V_m = \Omega(V_y)$  and the maximum displacement due to structure deformation as  $u^u = \mu u^y = \mu(V_y/K)$ , total maximum displacement yields to (Eq. (7))

$$\begin{aligned} u_t^u &= \frac{\mu V_y}{K} + \Omega \left( \frac{V_y}{K_x} + \frac{V_y(H_e)^2}{K_r} \right) \\ &= V_y \left[ \frac{\mu}{K} + \Omega \left( \frac{1}{K_x} + \frac{(H_e)^2}{K_r} \right) \right] \end{aligned} \quad (7)$$

Substituting on Eq. (2), equivalent ductility can be expressed as (Eq. (8))

$$\tilde{\mu} = \frac{u_t^u}{u_t^y} = \frac{\left[ \frac{\mu}{K} + \Omega \left( \frac{1}{K_x} + \frac{(H_e)^2}{K_r} \right) \right]}{\left[ \frac{1}{K} + \frac{1}{K_x} + \frac{(H_e)^2}{K_r} \right]} \quad (8)$$

Elastic stiffness of the structure ( $K$ ) can be expressed in terms of the fixed base period ( $T$ ). Horizontal ( $K_x$ ) and rocking ( $K_r$ ) stiffness of the foundation can be expressed in terms of the period of the structure behaving as a rigid body in translation ( $T_x$ ) and rocking ( $T_r$ ) too. (Wolf, 1985) (Eq. (9))

$$T^2 = \frac{4\pi^2 M_e}{K}; \quad T_x^2 = \frac{4\pi^2 M_e}{K_x} \quad \text{and} \quad T_r^2 = \frac{4\pi^2 M_e H_e^2}{K_r} \quad (9)$$

Substituting Eq. (9) in Eq. (8), and using the definition of the equivalent period (Avilés and Pérez-Rocha 2004)  $\tilde{T}^2 = T^2 + T_x^2 + T_r^2$ , yields to (Eq. (10))

$$\begin{aligned} \tilde{\mu} &= \frac{[\mu T^2 + \Omega(T_x^2 + T_r^2)]}{[T^2 + T_x^2 + T_r^2]} = \left( \frac{T}{\tilde{T}} \right)^2 \left[ \mu + \Omega \frac{(\tilde{T}^2 - T^2)}{T^2} \right] \\ &= \left( \frac{T}{\tilde{T}} \right)^2 (\mu - \Omega) + \Omega \end{aligned} \quad (9)$$

For elastoplastic systems ( $\Omega = 1$ ) Eq. (10) yields to Eq. (1). This proposed equation takes into account the post yield stiffness of the structure only by using the equivalent period and the overstrength of the structure. Previous studies have found that overstrength is not influenced by base flexibility (Fernández-Sola *et al.* 2015). Avilés and Pérez-Rocha (2011) proposed an equation in terms of explicit post yield stiffness of the system. Nevertheless, in the design process, the overstrength factor is used more commonly than the post yield stiffness. Expressing post yield stiffness in terms of  $\Omega$  and  $\mu$ , the equation proposed by Avilés and Pérez-Rocha (2011) yields to the equation proposed in this work. Many building codes defines overstrength as the ratio of maximum shear and design shear ( $\Omega_D = V_u/V_D$ ). Under these conditions,  $\Omega_D$  values included on building codes are larger than the values used in the present work which consider  $V_y$  instead of  $V_D$ . It is necessary to explore the relation between  $V_y$  and  $V_D$  in different structural systems in order to establish the ratio  $\Lambda_\Omega = \Omega/\Omega_D$  used in Eq. (10). Expressing Eq. (10) in terms of  $\Omega_D$  yields to:

$$\tilde{\mu} = \left( \frac{T}{\tilde{T}} \right)^2 (\mu - \Lambda_\Omega \Omega_D) + \Lambda_\Omega \Omega_D \quad (9)$$

Variations of equivalent ductility estimated with Eq. (10) are shown on Fig. 3. Equivalent ductility ( $\tilde{\mu}$ ) was computed for bilinear systems with different fixed base ductility ( $\mu = 1.5, 2, 3$  and  $4$ ) and overstrength factors

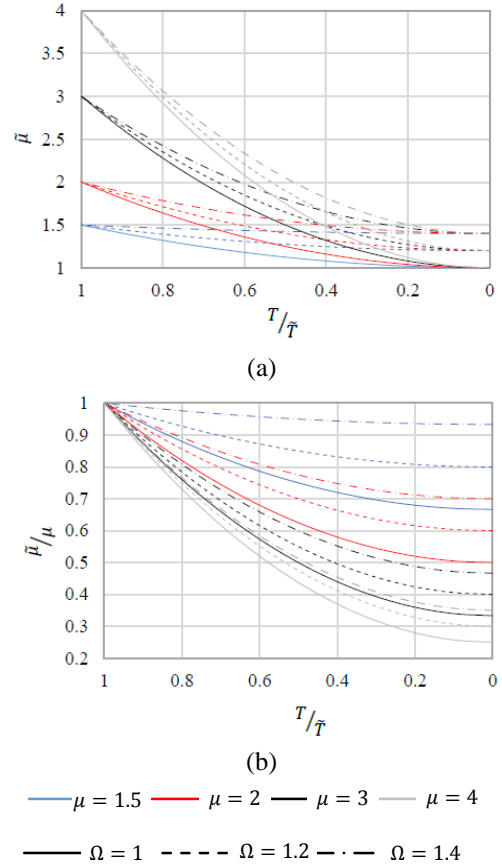


Fig. 3 (a) Equivalent ductility ( $\tilde{\mu}$ ) variation and (b) ductility reduction for bilinear systems with different overstrength factors ( $\Omega$ )

( $\Omega = 1, 1.2$  and  $1.4$ ). Results are plotted in terms of the period shift due to base flexibility ( $T/\tilde{T}$ ). Equivalent ductility is shown on figure 3(a). For the fixed base case ( $T/\tilde{T} = 1$ ) all systems yield to the fixed base ductility, regardless of  $\Omega$ , as expected. As base becomes more flexible, equivalent ductility decreases. Values of equivalent ductility are smaller for perfectly elastoplastic systems ( $\Omega = 1$ ) in all cases. This means that the use of Eq. (1) can be conservative. As  $\Omega$  becomes larger, values of equivalent ductility get larger. For the theoretical case of a infinitely flexible base ( $T/\tilde{T} = 0$ ),  $\tilde{\mu}$  yields to  $\Omega$  in all cases. For bilinear systems, this results represent elastic behavior of the system. On Fig. 3(b), results are shown as the ratio of equivalent ductility and fixed base ductility ( $\mu/\tilde{\mu}$ ). As fixed base system ductility becomes larger, reductions of equivalent ductility are larger too. Again, it can be seen that the greater reductions are associated with systems with ( $\Omega = 1$ ). In fact, reductions on the system with  $\mu = 3$  and  $\Omega = 1$  are slightly larger than the reductions on the system with  $\mu = 4$  and  $\Omega = 1.4$ . This effect is more pronounced for the systems with  $\mu = 1.5$  and  $\Omega = 1$  and  $\mu = 2$  and  $\Omega = 1.4$ . So ductility reductions estimated with the elastoplastic approach can be very conservative.

#### 4. Case of study

Table 1 Soil-structure parameters

$V_s$ (m/s)	$\bar{T}$ (s)	$K_h$ (t/m)	$K_r$ (t · m)	$\zeta_h$ (%)	$\zeta_r$ (%)	$\zeta_e$ (%)
$\infty$	0.83	$\infty$	$\infty$	0	0	5
250	0.87	$2.37 \times 10^5$	$3.02 \times 10^7$	3.1	2.5	4.6
100	1.08	$3.72 \times 10^4$	$4.50 \times 10^6$	22.1	2.6	4.9
70	1.36	$1.77 \times 10^4$	$2.09 \times 10^6$	25.6	0.23	4.6

In order to assess the accuracy of ESDOF approach, a 10 story RC building was analyzed. The building was designed following the procedure described on the Mexico City Building Code (MCBC 2004). Dimensions of the elements and details of the design can be found on Huerta-Écatl (2015). Representative diagrams of buildings are shown on Fig. 4. RC moment resistant frames designed with moderate ductility criteria ( $\mu=2$ ) accordingly to MCBC are used. Fundamental period of the building with fixed base is  $T=0.83$  s. The supporting soil corresponds to a homogeneous layer with thickness of  $H_s=40$  m. Three soil types with different stiffness are considered ( $V_s=70, 100$  and  $250$  m/s) in addition to the fixed base model ( $V_s=\infty$ ). Foundation consists on a mat foundation overlaying this homogenous soil layer. The foundation is embedded 5 m for all soil types.

Base flexibility is taken into account with the dynamic stiffness of the soil-foundation system (impedance function) as presented by Gazetas (1991). A set of distributed springs along mat foundation is used (Fig. 4). This procedure considers the influence of the soil mass and stiffness, so the dynamic stiffness of the soil-foundation system depends on the frequency of the excitation. Since a static and time domain analysis were performed, only the value of the impedance functions corresponding to the fundamental frequency of the soil-structure system was used. Given that the period of the soil-structure system with flexible base ( $\bar{T}$ ) and base flexibility are mutually dependent, it is necessary to perform an iterative process to establish the definitive values of impedance functions. DYNA6 software (Novak *et al.* 2012) was used to estimate the values of impedance functions in horizontal and rocking direction. Soil-foundation stiffness ( $K_x$  and  $K_r$ ) and periods of the structure with fixed and flexible base are presented on Table 1.

Additional damping introduced by DSSI is taken into account by using an effective damping ratio. Effective damping ratio was computed with the procedure included on MCBC (2004).

The main limitation of using equivalent springs with a constant stiffness is that the dependence of the impedance functions with frequency is partially considered. In order to establish the accuracy of the SSI model used, the response on the softest soil compared with the results computed with a frequency domain method model. This model considers directly the dependence of the impedance functions with frequency. The frequency domain model is based on computing the transfer function of the soil-structure system, solving the equation of motion in the frequency domain. Each story is represented by its horizontal displacement, with lumped mass (shear model). Soil foundation stiffness

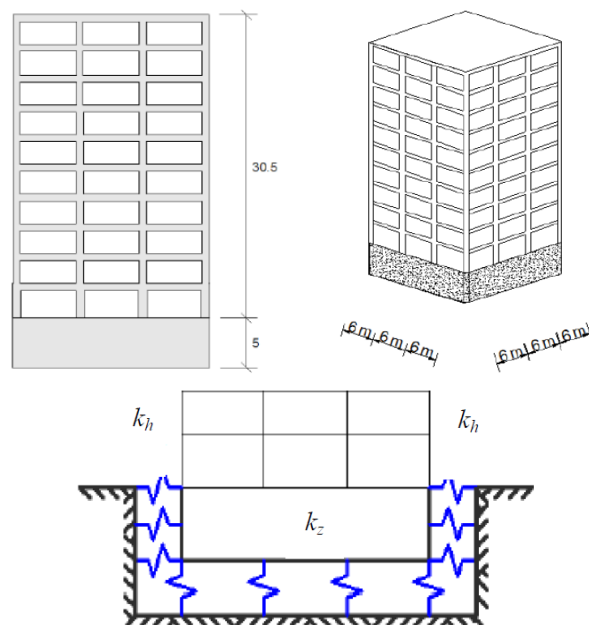


Fig. 4 Building scheme and base flexibility model

is considered incorporating two degrees of freedom (translation and rotation) and, coupling the impedance functions values in the stiffness and damping matrix for the global system. In the mass matrix, the masses associated with inertial forces that will produce rigid body motions of the superstructure must be included due to the base flexibility. Since non linear behavior is considered exclusively on the elements of the structure, and frequency domain models can not include non linear behavior, only the elastic response is compared. More details of the formulation of this model may be found in Avilés (1990), Fernández-Sola and Avilés (2008).

To reproduce the shear model on the structural model, rigid beams and axially rigid columns were considered for comparing with the frequency domain model. On the non linear analysis presented below, beams are considered flexible as well as the columns in the axial direction. On the frequency domain model, kinematic interaction is considered multiplying the Fourier spectrum of the free field motion by the transfer functions proposed by Kausel *et al.* (1978). Both, translational and rotational effective motions produced by kinematic interaction are considered.

Time history displacements on three different stories representing the low, middle and high part of the structure (1, 5 and 10) are shown on Fig. 5. Structure was subjected to September 19th 1985 Mexico City earthquake recorded on a soft soil (Fig. 6). Only the strong motion phase is shown in order to have a better comparison. The general trend on both models is very similar, indicating that the frequency content of the response is well reproduced by the equivalent model. Magnitude of the displacements are slightly different. This trend is the same along structure height. In addition, peak floor displacements ( $u_{max}$ ) along all height is shown on Fig. 5. It can be seen that peak floor displacements are reasonably estimated with the equivalent model for the studied case. Peak floor displacements at 1st, 5th and 10th levels are pointed out on Fig. 5. Studied models

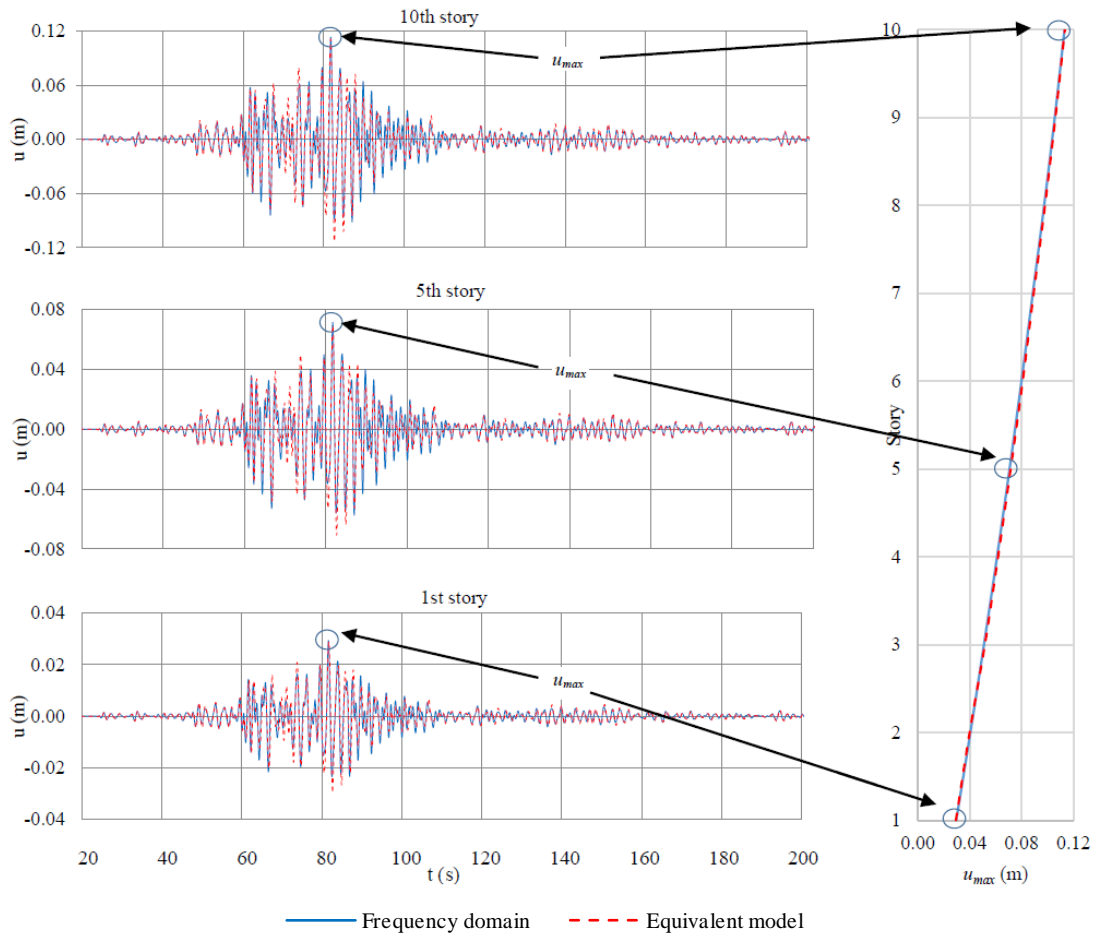


Fig. 5 Displacements computed with the frequency domain model and the equivalent model

are very regular in plain and height, so their response is highly controlled by the fundamental mode (the mass ratio for fundamental period is 85%).

Since soil-foundation stiffness used on the equivalent model were computed for the fundamental mode of the soil-structure system, responses are very similar. For structures with larger higher modes contributions, the equivalent model approach must not be so accurate. For those cases, lumped mass models for SSI consideration must be more suitable (Wolf 1994).

On the other hand, soil stiffness and foundation depth ( $D$ ) produce that kinematic effects are small for the studied case. Kausel *et al.* (1978) established that kinematic effects become important for high frequency motions. These motions can be identified with a simplified threshold defined by an equivalent frequency  $f_e = 0.7 V_s / (4D)$ . For the studied cases,  $f_e$  values are 8.75 Hz ( $T_e = 0.11$  s), 3.5 Hz ( $T_e = 0.29$  s) and 2.45 Hz ( $T_e = 0.41$  s) for  $V_s = 250$ , 100 and 70 m/s respectively. Ground motions correspond to real earthquakes. For each soil type, a different excitation was used in order to consider the differences on ground motion produced by soil type (site effects). Records for  $V_s = 70$  and 100 m/s correspond to September 19<sup>th</sup> 1985 Mexico City earthquake on SCT and Viveros stations respectively. Record for  $V_s = 250$  m/s corresponds to October 9<sup>th</sup> 1995 Colima earthquake on Manzanillo station. On Fig. 6, accelerograms and elastic response spectra of the different

ground motions are shown. The interval of periods where kinematic effects are expected to be important is indicated with a grey band on the response spectrum. It can be seen that for all cases that kinematic effects are expected to be small, so on the numerical analysis free field motion was used as excitation.

Fundamental period of the structure with fixed (FB) and flexible base (DSSI) are indicated on each response spectra. In order to meet the spectral acceleration values considered on the code, excitation was scaled to meet spectral pseudo accelerations around 1 g for structures fundamental periods with fixed base.

Horizontal stiffness was uniformly distributed among 24 horizontal individual springs ( $k_x$ ). Rotational stiffness was distributed considering the contribution of the horizontal springs and 16 additional vertical individual springs ( $k_z$ ). Base of the first story columns are constrained with a master joint with a rigid body condition. More details of this procedure can be found on Huerta-Écatl (2015).

## 5. Numerical analysis and results

### 5.1 Pushover analysis

Static non-linear analysis is performed with triangular load pattern with displacement control. For the columns, the

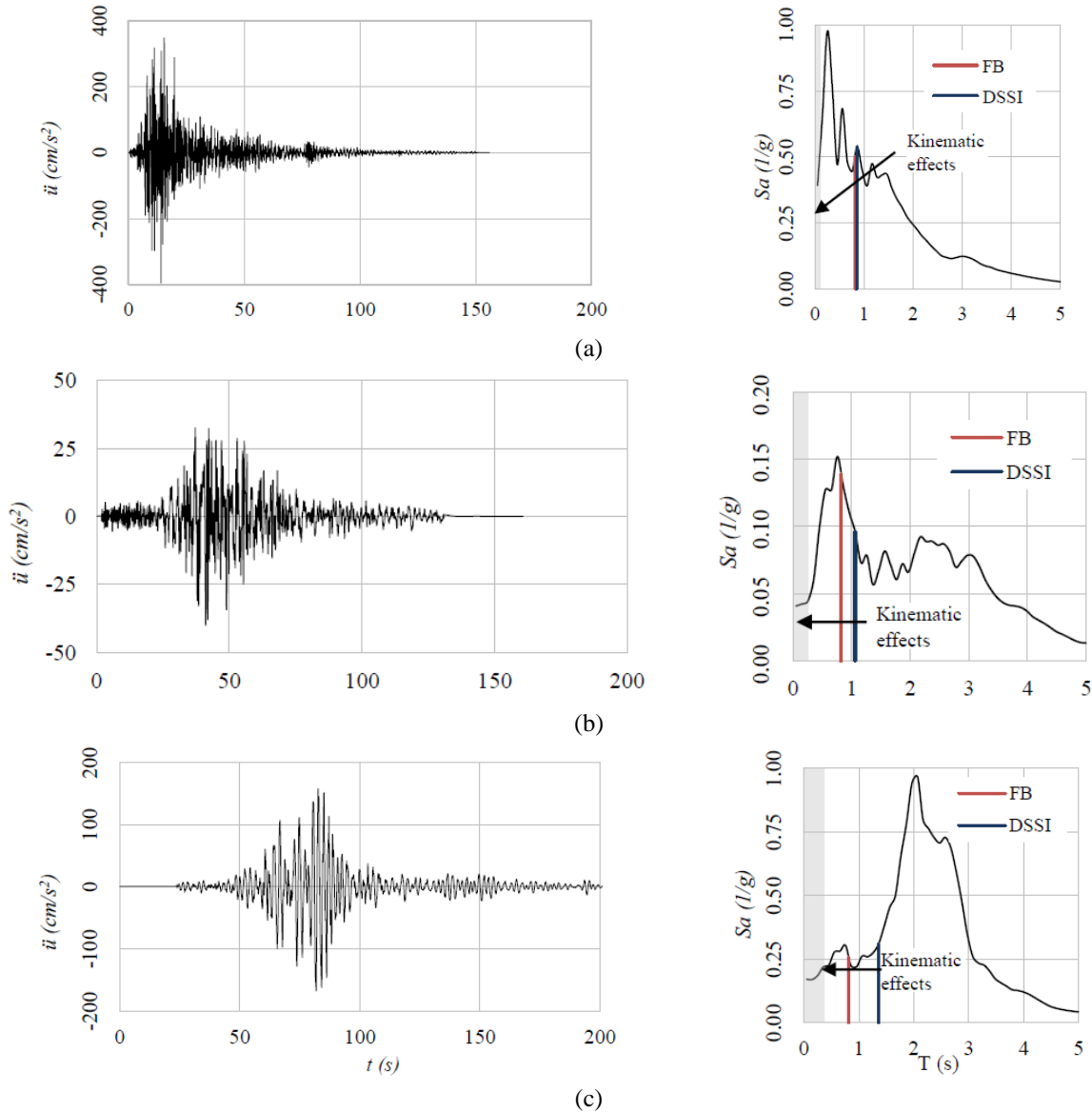


Fig. 6 Accelerograms and elastic response spectrum of the ground motions on different soil types (a)  $V_s=250$  m/s, (b)  $V_s=100$  m/s and (c)  $V_s=70$  m/s.)

Table 2 Non linear parameters of frame sections (beams and columns)

Story	Dimension (m)	$M_y$ (ton-m)	$M_u$ (ton-m)	$\mu_\phi = \frac{\phi_u}{\phi_y}$	$l_p$ (m)	$\theta_p$ (rad)	
Beams	1	0.50x0.70	81.85	87.52	7.35	0.40	0.01030
	2-6	0.45x0.70	90.58	97.79	6.66	0.40	0.00941
	7-10	0.40x0.70	63.25	65.76	9.71	0.40	0.01332
Columns	1	0.80x0.80	162.17	200.41	5.53	0.45	0.00724
	2-7	0.70x0.70	136.01	168.46	4.40	0.40	0.00594
	8-10	0.65x0.65	92.12	112.66	4.92	0.35	0.00625

influence of axial force on the non linear behavior is considered. The nonlinear parameters for the sections (yield moment ( $M_y$ ), maximum moment ( $M_u$ ), curvature ductility ( $\mu_\phi$ ), plastic length ( $l_p$ ) and plastic rotation ( $\theta_p$ )) are reported on Table 2. The possibility of plastic hinges is

defined at 5 and 95 percent of the length for frame elements. Plastic length is computed with the empiric equation proposed by Park and Paulay (1974).

Overall capacity curves, defined by the relation between the base shear and the average drift are presented in Fig. 7. The average drift is estimated as the ratio of the displacement of the top of the building and building total height. Maximum displacement is defined when one of the following three conditions is achieved: a) a plastic hinge develops a rotation greater than the maximum rotation feasible for that element; b) all columns of the same story develop plastic hinges at both ends, producing a soft story failure mechanism and c) all element ends that concur at one joint develop plastic hinges, producing a joint plastic mechanism.

Ductility on buildings with fixed and flexible base were estimated with two sets of results. First, the capacity curves consider the total displacement which includes both the

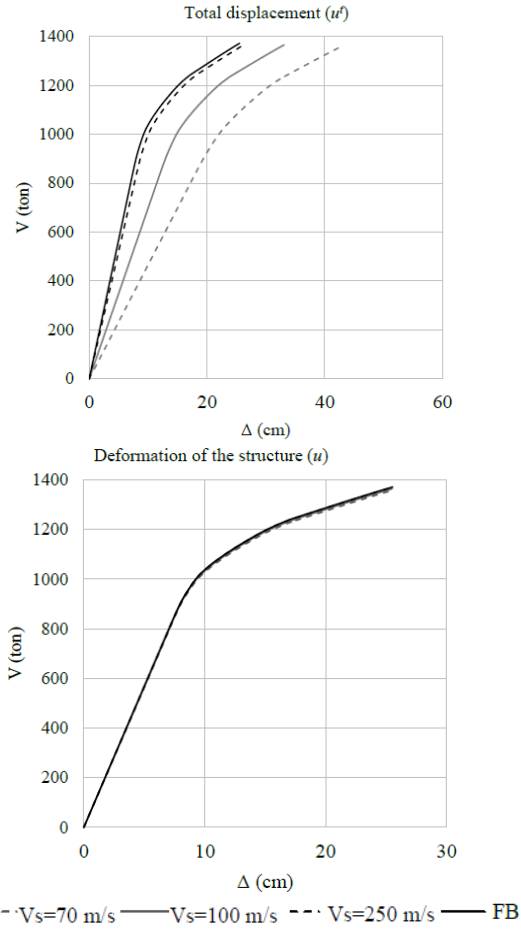


Fig. 7 Capacity curves of the building on different soils (FB,  $V_s=250, 100,$  and  $70$  m/s) with total displacement (left) and structure deformation (right)

displacement associated with structure deformation ( $u$ ) and the displacement produced by rigid body behavior ( $u_x$  and  $\theta$ ). This set of results are computed to compare the inelastic parameters of the multistory building with the equivalent properties proposed by the ESDOF approach. The second set of capacity curves consider only the displacement associated with structure deformation ( $u$ ). This results are used to establish if the inelastic parameters of the structure are modified by base flexibility due to  $P-\Delta$  effects.

From capacity curves, yield and maximum shear and the corresponding displacements were estimated. Ductility is defined as the ratio of maximum displacement and yield displacement. On Table 3, ductility factors for the structure with different soil types are shown. When total displacement is considered, base flexibility reduces the developed ductility, which computed in this way correspond to equivalent ductility previously defined ( $\tilde{\mu}$ ). This ductility reduction is associated with the increment of yield displacement, as previously discussed. As soil becomes more flexible, ductility reduction increases. On the other hand, when only the displacement associated with structure deformation is considered ( $\mu$ ), ductility remains constant for all cases. This is an expected result, since the inelastic capacity of the building must be independent on the base condition if  $P-\Delta$  effects are small enough to not change

Table 3 Structure ductility ( $\mu$ ) and equivalent ductility computed with different approaches ( $\tilde{\mu}$ =from the capacity curve,  $\tilde{\mu}_{eq.1}$ =elastoplastic system,  $\tilde{\mu}_{eq.5}$ =considering explicitly the displacement components and  $\tilde{\mu}_{eq.10}$ = using  $\Omega$ )

$V_s$ (m/s)	Ductility capacity				
	$\mu$	$\tilde{\mu}$	$\tilde{\mu}_{eq.1}$	$\tilde{\mu}_{eq.5}$	$\tilde{\mu}_{eq.10}$
$\infty$ (FB)	2.67	2.67	2.67	2.67	2.67
250	2.67	2.54	2.50	2.54	2.54
100	2.67	2.12	2.00	2.15	2.09
70	2.67	1.85	1.66	1.89	1.78

Table 4 Displacement components for yield and maximum displacements ( $u_t^y$  and  $u_t^u$ )

$V_s$ (m/s)	$T/\tilde{T}$	$\Omega$	Displacement components at $u_t^y$ (%)			Displacement components at $u_t^u$ (%)		
			$u_x^y$	$\theta^y(H_e + D)$	$u^y$	$u_x^u$	$\theta^u(H_e + D)$	$u^u$
$\infty$ (FB)	1.000	1.25	-	-	100.00	-	-	100.00
250	0.954	1.25	0.56	7.71	91.73	0.28	3.87	95.85
100	0.769	1.25	2.17	35.83	62.00	1.31	21.69	77.00
70	0.610	1.25	2.77	55.15	42.08	1.94	38.54	59.52

structures behavior (Fernández-Sola *et al.* 2015). Buildings studied in the present work exhibit this behavior. In addition, effective ductility ( $\tilde{\mu}$ ) computed with Eqs. (1), (5) and (10) are reported on Table 3 ( $\tilde{\mu}_{eq.1}, \tilde{\mu}_{eq.5}$  and  $\tilde{\mu}_{eq.10}$ ). Contribution of the different displacement components to yield and maximum total displacement are reported on Table 4 as well as period shift and overstrength factor,  $\Omega = V_u/V_y$ . For the studied cases  $\Omega$  remains constant independently of the soil stiffness.

Equivalent ductility computed with Eq. (1) (elastoplastic system) is smaller than the ductility from the capacity curves for all cases. Difference becomes larger as soil stiffness is reduced. As discussed on section 2, results from elastoplastic approach corresponds to a lower boundary for  $\tilde{\mu}$  since overstrength is neglected. On the other hand, equivalent ductility computed with Eq. (5) and (10), which considers the overstrength of the structure, yields to similar values to the ones computed from the capacity curves. In general, for the studied cases, Eq. (5) tends to slightly overestimate equivalent ductility while  $\tilde{\mu}$  estimated with Eq. (10) are smaller. From this results, it can be said that ESDOF approach represents in an accurate way the global ductility of the multiple degree of freedom system, specially when overstrength is considered. This result is in good agreement to the study presented by Ganjavi and Hao (2011).

### 5.2 Non linear time history analysis

Non linear dynamic analysis was performed for the structures with fixed and flexible base. As mentioned before, ground motions were selected to be coherent with the soil properties considered for the flexible base models,

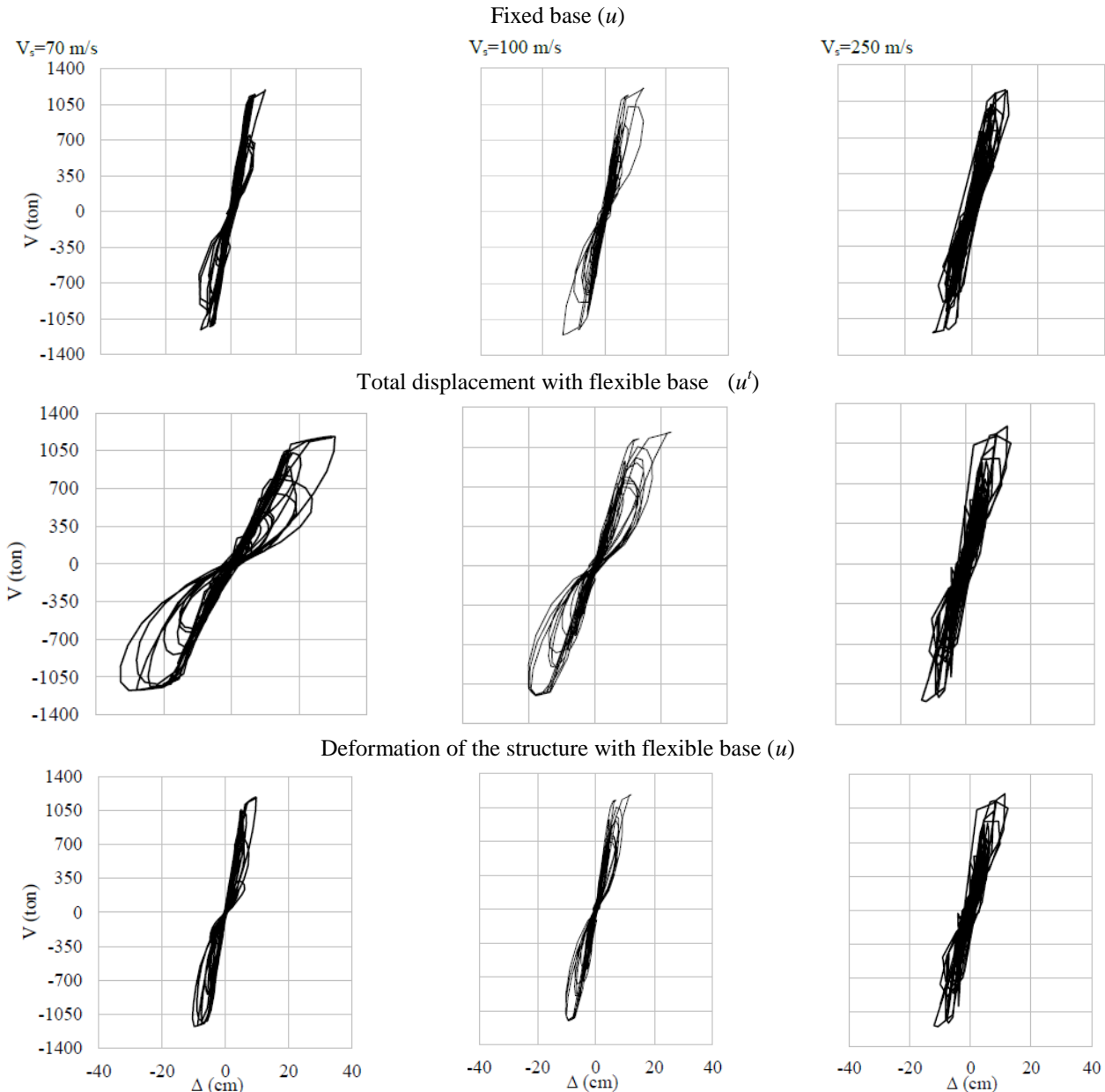


Fig. 8 Capacity curves of the building on different soils (FB,  $V_s=250, 100,$  and  $70$  m/s) with total displacement (left) and structure deformation (right)

to take into account for the site effects. Global and local ductility demands were computed by non linear time history analysis. For global behavior, as well as in the pushover analysis, two types of results were computed for the buildings with flexible base, one considering the total displacement and other considering only the structure deformation. For the analysis of element ductility, only its deformation is considered.

Non linear parameters for elements (beams and columns) are the same as for the pushover analysis. The hysteretic model proposed by Takeda (1970) is used to consider stiffness degradation. Analysis is performed for the whole duration of the excitation, since none of the elements achieves its maximum plastic rotation in any moment. Only inelastic behavior for flexure is considered given that design procedure considers that shear failure is avoided.

Global base shear-displacement curves are shown on Fig. 8 for fixed and flexible base, considering the roof displacement. Yield and maximum displacements are presented on Table 5. In this table, total displacement ( $u^t$ ) and structure deformation ( $u$ ) for the system with flexible base (DSSI) are reported. For fixed base (FB), total displacement is equal to the structure deformation.

Three different ductility demands are computed. For FB, ductility demand is computed directly by the ratio of maximum to yield displacement ( $\mu_{FB} = u_{FB}^u / u_{FB}^y$ ). This value corresponds to the ductility demand on the structure neglecting the DSSI. For flexible base, demand of the whole system is computed as the ratio of total maximum to total yield displacements ( $\tilde{\mu}_{DSSI} = u_{uDSSI}^t / u_{yDSSI}^t$ ). In addition, ductility demand on the structure is defined as the ratio of maximum and yield displacements associated with

Table 5 Total displacement and structure deformation for yield and maximum displacements with fixed and flexible base

Response with fixed base				Response with flexible base					
$V_s$ (m/s)	$u_{FB}^y$ (cm)	$u_{FB}^u$ (cm)	$\mu_{FB}$	$u_{yDSSI}^t$ (cm)	$u_{uDSSI}^t$ (cm)	$\tilde{\mu}_{DSSI}$	$u_{yDSSI}$ (cm)	$u_{uDSSI}$ (cm)	$\mu_{DSSI}$
250	7.60	11.98	1.58	8.33	13.73	1.65	7.32	12.20	1.67
100	5.43	13.61	2.51	10.60	23.18	2.19	5.26	12.16	2.31
70	5.71	10.73	1.88	18.91	33.08	1.75	5.83	10.52	1.80

the deformation of the structure ( $\mu_{DSSI} = u_{uDSSI}/u_{yDSSI}$ ). This value corresponds to the target ductility demand of the design.

When total displacement is considered, the displacements of the system with flexible base are larger due to increased flexibility as expected. The increment on maximum total displacement is of 15, 70 and 208% for  $V_s=250$ , 100 and 70 m/s respectively (Table 5). This is an important effect to verify possible collision with adjacent buildings, and the response of contents (Jaimes-Téllez *et al.* 2017). On the other hand, the displacements produced by deformation of the structure can be increased or reduced. For  $V_s=100$  m/s, yield and maximum displacements are reduced by base flexibility. For  $V_s=250$  m/s yield displacement is reduced but maximum displacement is increased, producing an increment on the ductility demand. The opposite happens for  $V_s=70$  m/s, where the yield displacement is increased while maximum displacement is reduced.

Because of this effect, ductility demands on the structure (Table 5) are modified by base flexibility, in some cases are increased ( $V_s=250$  m/s) and in other cases reduced ( $V_s=100$  and 70 m/s). This is a confirmation that DSSI does not always reduces the structural response. The increase or reduction of structural response largely depends on the spectral shape of the excitation, on the period shift and on the variation of the inelastic response produced by DSSI. As for the pushover analysis, ductility demands on the structure ( $\mu_{DSSI}$ ) are larger than global ductility computed with total displacements ( $\tilde{\mu}_{DSSI}$ ), for all cases. However, the larger increment is for  $V_s=100$  m/s, and not for the most flexible soil ( $V_s=70$  m/s).

The design procedure of inelastic structures is based on setting specific values of  $R_\mu$  to achieve a target ductility demand. Since  $\mu_{DSSI}$  is always larger than  $\tilde{\mu}_{DSSI}$ , it is necessary to use reduced  $R_{\mu DSSI}$  values to keep  $\mu_{DSSI}$  within design values. Variations of  $R_\mu$  values are analyzed. Maximum base shear ( $V_u$ ) and base shear of the corresponding linear system ( $V_0$ ) and  $R_\mu$  values are shown on Table 6. Since the same design is considered for all cases, yield base shear remains constant ( $V_y = 1,100$  t). Maximum shear ( $V_u$ ) is very similar for all excitations and all soil conditions given that the maximum base shear in the structure can be associated to its strength. Variations are produced on the  $R_\mu$  magnitudes, due to modification of  $V_0$ . For  $V_s=250$  and 100 m/s,  $R_\mu$  are larger for the system with fixed base, while for  $V_s=70$  m/s, reduction factor is larger

Table 6 Maximum base shear for the inelastic ( $V_u$ ) and corresponding linear system ( $V_0$ ) and yield strength reduction factors ( $R_\mu$ ) with fixed (FB) and flexible base (DSSI)

Response with fixed base				Response with flexible base			
$V_s$ (m/s)	$V_{uFB}$ (ton)	$V_{0FB}$ (ton)	$R_{\mu FB}$	$V_{uDSSI}$ (ton)	$V_{0DSSI}$ (ton)	$R_{\mu DSSI}$	$V_{uFB}/V_{uDSSI}$
250	1,161	3,493	3.18	1,203	3,758	3.41	0.97
100	1,206	3,013	2.74	1,182	2,138	1.94	1.02
70	1,195	1,818	1.65	1,179	2,514	2.29	1.01

with flexible base.

A fundamental parameter is the ductility demand ( $\mu$ ) associated with  $R_\mu$ . The ratio of  $R_\mu/\mu$  was computed for the different systems (Table 7). For  $V_s=250$  and 100 m/s,  $R_\mu/\mu$  are smaller for the flexible base system. This means that base flexibility produces larger ductility demand for a specific reduction on the yield strength. On the other hand, for  $V_s=70$  m/s,  $R_\mu/\mu$  is larger for the flexible base system. Variations depend partially on the spectral shape and the spectral position of the fundamental periods of the structure (Ruiz-García and Miranda 2004, Chopra 2012). However, the appearance of displacements due to rigid body behavior has an influence on the modification of this ratio too.

To study this effect, the ratio in terms of equivalent ductility ( $\tilde{\mu}_{DSSI}$ ) is presented on Table 7. As mentioned above,  $\tilde{\mu}$  does not separate the displacement produced by the deformation of the structure of the displacement produced by rigid body behavior, so this is a virtual ductility demand, which is used for design purposes. As shown on Table 5,  $\tilde{\mu}_{DSSI}$  is smaller than  $\mu_{DSSI}$  in all cases, so  $R_\mu/\tilde{\mu}_{DSSI}$  is consistently larger than  $R_\mu/\mu_{DSSI}$ . On the design process, the ratio of strength reduction and ductility demand is defined based on the definition of ductility of Eq. (2), so the design target ductility demand ( $\tilde{\mu}_{DSSI}$ ) and the actual ductility demand on the structure ( $\mu_{DSSI}$ ) are not equal. In order to illustrate the differences of design strength yield reduction factor for the systems with fixed and flexible base, the corresponding  $R_\mu$  for a target ductility demand on the structure of  $\mu = 2$  are computed (Table 7). For flexible base two  $R_\mu$  are computed, one using  $\tilde{\mu}$  and other with  $\mu$ . If global ductility of  $\tilde{\mu} = 2$  is used, corresponding  $R_\mu$  are larger than the actual values that must be used to get a target ductility demand of  $\mu = 2$  on the structure. For  $V_s=250$  and 100 m/s, the required values of  $R_\mu$  are smaller for flexible base. The opposite happens for  $V_s=70$  m/s, where the  $R_\mu$  factor is greater for the flexible base system. For this reason, some building codes considers reduced values of inelastic capacity of systems with flexible base for the computation of yield strength reduction factors.

Equivalent ductility computed with Eq. (1), (5) and (10) for dynamic analysis are reported on Table 8 and compared with values computed directly from response of the structure used as reference (Table 5). The contribution of each displacement component in percentage for use of Eq. (5) are reported too. Developed overstrength ( $\Omega$ ), computed

Table 7 Ratio of  $R_{\mu} / \mu$  and ductility variation for systems with fixed (FB) and flexible base (DSSI)

$V_s$ (m/s)	$R_{\mu FB}$ $/\mu_{FB}$	$R_{\mu DSSI}$ $/\mu_{DSSI}$	$R_{\mu DSSI}$ $/\mu_{DSSI}$	$R_{\mu DSSI}$ $/\mu_{FB}$	$\mu_{DSSI}$ $/\mu_{DSSI}$	For $\mu = 2$		
						$R_{\mu FB}$	$R_{\mu DSSI}$	$R_{\mu DSSI}$
250	2.01	1.93	1.90	1.06	1.01	4.02	3.86	3.80
100	1.09	0.89	0.84	0.92	1.05	2.18	1.78	1.68
70	0.88	1.31	1.27	0.96	1.03	1.76	2.62	2.54

Table 8 Displacement components for yield and maximum displacements ( $u_t^y$  and  $u_t^u$ )

$V_s$ (m/s)	Displacements at $u_y$		Displacements at $u_u$		$\Omega = V_u/V_y$	$\tilde{\mu}$	$\tilde{\mu}_{eq.1}$	$\tilde{\mu}_{eq.5}$	$\tilde{\mu}_{eq.10}$
	$u_{RB}^y$ (%)	$u_{RB}^u$ (%)	$u^y$ (%)	$u^u$ (%)					
250	12.12	11.14	87.88	88.86	1.06	1.65	1.59	1.65	1.62
100	50.38	47.54	49.62	52.46	1.10	2.19	1.70	2.19	1.82
70	69.17	68.20	30.83	31.80	1.09	1.75	1.28	1.75	1.35

as the ratio of maximum base shear developed on the structure and the yield base shear ( $\Omega = V_u/V_y$ ) is used for Eq. (10) (Table 8). As for pushover analysis, values of equivalent ductility computed with Eq. (1) are the smallest. Values computed from Eq. (5) are equal to the values computed directly from the response of the structure in this case, in difference to the pushover analysis where values are similar but not equal. On the other hand, values computed with Eq. (10) are closer to the reference values than the values of Eq. (1). However, in this case these values are significantly smaller. With these results it can be confirmed that neglecting the post-yield stiffness may lead to large errors on predictions of global ductility.

Rotational ductility demands on beams were computed as the ratio of maximum to yield rotation. Demands on an external (EB) and internal beam (IB) in an external (EF) and internal frame (IF) on each floor are analyzed (Fig. 9). In order to study the modification on ductility demand

produced by DSSI, the ratio of ductility demand with fixed and flexible base is presented ( $\mu_{\theta DSSI}/\mu_{\theta FB}$ ) on Fig. 10. The dotted red line corresponds to values of  $\mu_{\theta DSSI}/\mu_{\theta FB} = 1$  (no change on ductility demand). Values greater than unit represent that base flexibility increases the ductility demand while smaller values represent a reduction of ductility demand. Results for the four different beams (EB-EF, IB-EF, EB-IF and IB-IF) along structure height and the average at each floor are shown on Fig. 10 (a), (b) and (c). Comparison of the average values for the different cases is shown on Fig. 10(d).

Modifications of ductility demand are different along structure height in all cases. Variations along height can not be reproduced with an ESDOF system. For  $V_s=70$  m/s, ductility demands on the 3<sup>rd</sup> story are reduced by base flexibility while for the 4<sup>th</sup> story, demands are increased. Actually, modifications of ductility demand are different in the different beams of the same story. For example, increment of ductility demand on the beams of the internal frame (IF) are larger than in the ones of the external frame (EF) in the first six stories for  $V_s=100$  m/s. In fact, the beams of the same frame in the same floor experience increments and reductions on the ductility demand (i.e., EF beams of the 6<sup>th</sup> story for  $V_s=250$  m/s). A concentration of ductility demand can be observed on the external beam of the external frame (EF-EB) of the first story for  $V_s=70$  m/s while the other three beams on the same story develop a reduction on the ductility demand.

Variation of global ductility demand reported on Table 7 can be compared with the local variations. For  $V_s=100$  m/s, global ductility demand is reduced about 8% ( $\mu_{DSSI}/\mu_{FB}=0.92$ ) and all ductility demands on beams are consistently reduced by base flexibility. However, local ductility reductions are up to 20% on the external beam of the external frame (EF-EB) in the first story, and the average ductility modification on this story is about 16%. Average ductility modification for 2-8 stories are very close to the global values. Beams on upper stories (9-10) experience a very small or even null inelastic behavior in all cases. For

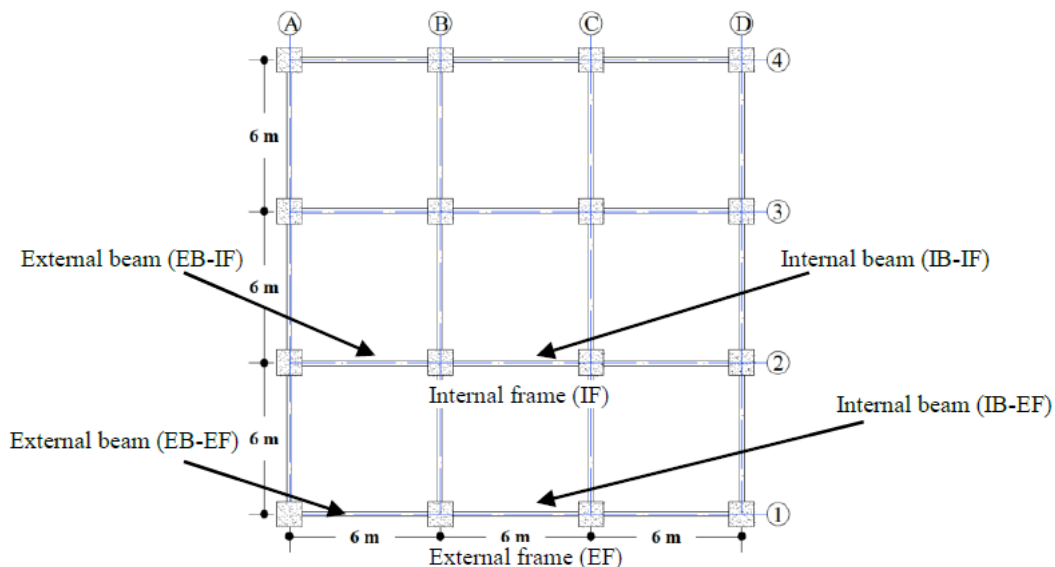


Fig. 9 Outline of frame and beam distribution on plain

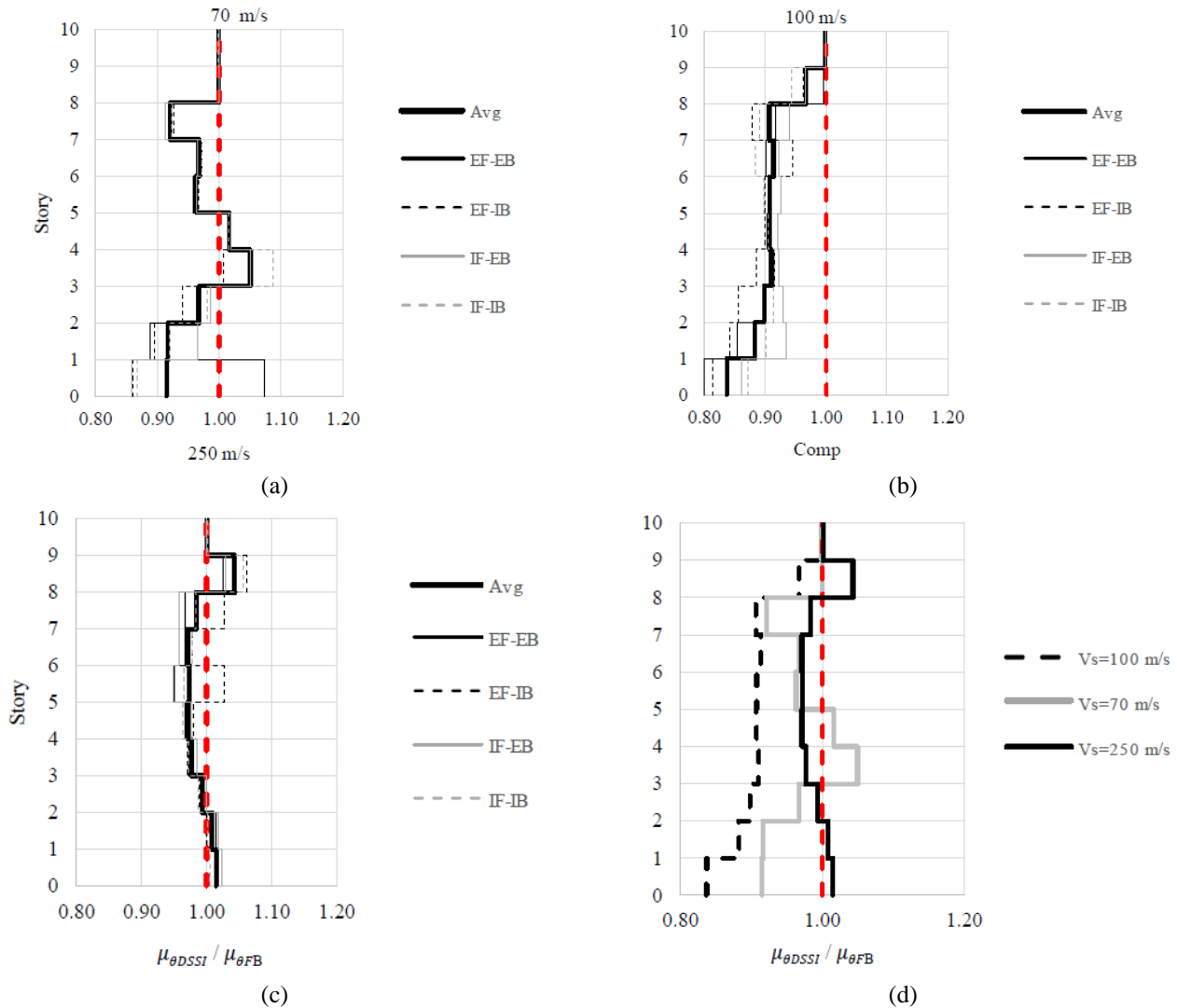


Fig. 10 Ratio of rotational ductility demands in each floor, on different beams (IB=internal and EB=external) of different frames (IF=internal and EF=external) of structures with flexible and fixed base ( $\mu_{\theta DSSI} / \mu_{\theta FB}$ ) with  $V_s=70, 100$  and  $250$  m/s

$V_s=250$  m/s, global ductility demand is increased about 6% as well as the average local ductility demand on the first two stories. In contrast, the ductility demand on the mid rise stories (3-8) is reduced by base flexibility. In this case, the global ductility modification is controlled by the variations on the lower stories. Previous studies had identified that the variation on inelastic response due to base flexibility on the first stories are the largest (Ghandil and Behnamfar 2017) and controls the global inelastic behavior of the structure (Fernández-Sola and Martínez-Galindo 2015). For  $V_s=70$  m/s, base flexibility reduces the global ductility demand about 4%. Again, the modification on lower stories (1-4) is consistent with the global ductility change, with reductions up to 9% for the first story. However, on 4<sup>th</sup> story, average ductility demand is increased in 5% with an increase on the internal beam of the internal frame (IF-IB) of 9%. It is clear that, even when the ESDOF approach used to take into account the variations of the DSSI predicts good approximation for the global ductility demand, the specific changes on the ductility demands on the elements may not be correctly computed, having in some cases increments on

local ductility demands while the ESDOF approach predicts reductions on the ductility demand.

## 6. Conclusions

Modification on the ductility of structures due to base flexibility is studied. The representation of the inelastic behavior of systems with flexible with an equivalent single degree of freedom system (ESDOF) is discussed as well as the role of the post yield stiffness. Two different equations for including the post yield stiffness effect on the ESDOF approach are proposed. One considers explicitly how the contribution of rigid body components influences the ductility modification and the other is based on the overstrength factor for design purposes. In order to exemplify the differences on the inelastic behavior of systems with fixed and flexible base the inelastic static and time history analysis of RC buildings with fixed and flexible base are presented. A moment resistant building with 10 stories is considered with a mat foundation.

Ductility capacities are defined based on the base shear-average drift capacity curves from the static non-linear analysis. Ductility demands and yield strength reduction factors are computed from time history non-linear analysis. Average drift was computed in two ways: one with the total displacement of the soil-structure system, which includes structure deformation and rigid body components, and other considering only the structure deformation. Impedance functions for the fundamental frequency are used.

From the static non-linear analysis, it is shown that ductility capacity computed with the displacement associated with structural deformation remains almost unchanged. It means that inelastic capacity of the structure remains equal independently on base flexibility. On the other hand, when total displacement is considered (whole soil-structure system), equivalent ductility is reduced by base flexibility in general. Ductility reduction in this case is mostly due to the increment on yield displacement produced by system flexibilization. Ductility reduction does not mean a reduction on deformation capacity, it is produced by the difference on the contribution of rigid body components to total displacement at yield and maximum displacement. Equivalent ductility computed from the capacity curves is compared with the values computed with the ESDOF approach considering elastoplastic behavior and the proposed equations. It is shown that values computed with the equations proposed in this work are more accurate than the ones computed considering an elastoplastic behavior.

Global ductility demand and the corresponding yield strength reduction factor are modified by base flexibility partially due to the change of fundamental period, and partially due to the appearance of rigid body displacements. For the flexible base structure, ductility demand on the whole soil-structure system (equivalent ductility) is smaller than the actual ductility demand produced on the structure. Values of the equivalent ductility demand computed from non linear time history analysis are compared with the ESDOF approach too. Proposed equations fits better numerical results of the global equivalent ductility than the elastoplastic approach. However, for the dynamic case, values computed with the proposed design equation based on the overstrength factor are not as accurate as the ones computed with the equation that considers the rigid body components. It is proved that the ratio between yield strength reduction factor and structure ductility demand is smaller for the structure with flexible base respect to the fixed base case.

The modification on rotational ductility demands on beams along the structure are presented. It is shown that ductility demands on beams are increased in some cases and decreased in others. Variations are not constant along the structure, effect that can not be reproduced with the ESDOF approach. For some cases, ductility demand on some beams are increased even when global ductility demand is reduced.

## Acknowledgments

Authors would like to acknowledge the grant given by Consejo Nacional de Ciencia y Tecnología (CONACyT) of

México for the master degree studies of second author and the comments given by Prof. Manuel Ruiz-Sandoval to improve the present paper.

## References

- ASCE 7 (2010), Minimum Design Loads for Buildings and Other Structures, ASCE Standard ASCE/SEI 7-10, American Society of Civil Engineers.
- Avilés, J. (1991), "Respuesta sísmica de un sistema suelo-estructura", *Revista Internacional de Métodos Numéricos para Cálculo y Diseño en Ingeniería*, **7**(1), 29-43. (in Spanish)
- Avilés, J. and Perez-Rocha, L.E. (2005), "Soil-structure interaction in yielding systems", *Earthq. Eng. Struct. Dyn.*, **32**(11), 1749-1771.
- Avilés, J. and Perez-Rocha, L.E. (2011), "Bases para las nuevas disposiciones reglamentarias sobre la interacción dinámica suelo estructura", *Revista de Ingeniería Sísmica*, **71**, 1-36. (in Spanish)
- Avilés, J. and Perez-Rocha, L.E. (2011), "Use of global ductility for design of structure-foundation systems", *Soil Dyn. Earthq. Eng.*, **31**, 1018-1026.
- Aydemir, M.E. and Ekiz, I. (2013), "Soil-structure interaction effects on seismic behaviour of multistorey structures", *Eur. J. Environ. Civil Eng.*, **17**(8), 635-653.
- Barcena, A. and Esteva, L. (2007), "Influence of dynamic soil-structure interaction on the nonlinear response and seismic reliability of multistorey systems", *Earthq. Eng. Struct. Dyn.*, **36**(3), 327-346.
- Chopra, A.K. (2012), *Dynamics of Structures*, 4th Edition, Prentice Hall, New Jersey.
- Eser, M., Aydemir, C. and Ekiz, I. (2011) "Effects of soil-structure interaction on strength reduction factors", *Procedia Eng.*, **14**, 1696-1704.
- Fernández-Sola, L.R. and Avilés, J. (2008) "Efectos de interacción suelo-estructura en edificios con planta baja blanda", *Revista de Ingeniería Sísmica*, **79**, 71-90. (in Spanish)
- Fernández-Sola, L.R. and Martínez-Galindo, G. (2015), "Behavior of RC frames with hysteretic dampers considering dynamic soil structure interaction", *11<sup>th</sup> Canadian Conference on Earthquake Engineering*, Victoria, BC, Canada.
- Fernández-Sola, L.R., Dávalos-Chávez, D. and Tapia-Hernández, E. (2014) "Influence of the dynamic soil structure interaction on the inelastic response of steel frames", *10th U.S. National Conference on Earthquake Engineering*, Anchorage, Alaska.
- Fernández-Sola, L.R., Tapia-Hernández, E. and Dávalos-Chávez, D. (2015), "Respuesta dinámica de marcos de acero con interacción inercial suelo-estructura", *Revista de Ingeniería Sísmica*, **92**, 1-21. (in Spanish)
- Ganjavi, B. and Hao, H. (2011), "Elastic and inelastic response of single- and multi-degree-of-freedom systems considering soil structure interaction effects", *Australian Earthquake Engineering Society 2011 Conference*, Barossa Valley, South Australia.
- Gazetas, G. (1991), *Foundation Vibrations*, Foundation Engineering Handbook, Ed. H.Y. Fang, Van Nostrand Reinhold.
- Ghandil, M. and Behnamfar, F. (2017), "Ductility demands of MRF structures on soft soils considering soil-structure interaction", *Soil Dyn. Earthq. Eng.*, **92**, 203-214.
- Ghannad, M.A. and Ahmadnia, A. (2006), "The effect of soil-structure interaction on inelastic structural demands", *Eur. Earthq. Eng.*, **20**(1), 23-35.
- Halabian, A.M. and Erfani, M. (2013), "The effect of foundation flexibility and structural strength on response reduction factor of

- RC frame structures”, *Struct. Des. Tall Spec. Build.*, **22**(1), 1-28.
- Huerta-Ecatl, J.E. (2015), “Evaluación de la interacción dinámica suelo-estructura en el comportamiento inelástico de un edificio de concreto reforzado”, Master Dissertation, Posgrado en Ingeniería Estructural, UAM-Azcapotzalco. (in Spanish)
- Jaimes-Tellez, M.A., Arredondo-Vélez, C.A. and Fernández-Sola, L.R. (2017), “Rocking of non-symmetric blocks in buildings considering effects associated with soil-structure interaction”, *J. Earthq. Eng.*, 1-28.
- Jarenpasert, S., Bazan-Zurita, E. and Bielak, J. (2013), “Seismic soil-structure interaction response of inelastic structures”, *Soil Dyn. Earthq. Eng.*, **47**, 132-143.
- Kausel, E., Whitman, R.V., Morray, J.P. and Elsabee, F. (1978), “The spring method for embedded foundations”, *Nucl. Eng. Des.*, **48**, 377-392.
- MCBC (2004), “Reglamento de construcciones para el Distrito Federal”, *Gaceta Oficial del Departamento del Distrito Federal*, México, México. (in Spanish)
- NBCC (2015), National Building Code of Canada, National Research Council of Canada, Ottawa.
- Novak, M., Sheta, M., El-Hifnawy, L., El-Marsafawi, H. and Ramadan, O. (2012), “DYNA6.1: A computer program for calculation of foundation response to dynamic loads”, Geotechnical Research Centre, The University of Western Ontario, Canada.
- NZS 3101-1 (2006), New Zealand Standard Code of Practice for General Structural Design and Design Loadings for Buildings, Standards Association of New Zealand, Wellington.
- Park, R. and Paulay, T. (1974), *Reinforced Concrete Structures*, 1st Edition, John Wiley & Sons.
- Rosenblueth, E. and Resendiz, D. (1988), “Disposiciones reglamentarias de 1987 para tener en cuenta interacción dinámica suelo-estructura”, *Series del Instituto de Ingeniería*, **509**, Universidad Nacional Autónoma de México, México. (in Spanish)
- Ruiz-García, J. and Miranda, E. (2004), “Inelastic displacement ratios for design of structures on soft soil sites”, *J. Struct. Eng.*, ASCE, **130**(12), 2051-2061.
- Takeda, T.M., Sozen, M.A. and Nielsen, N.N. (1970), “Reinforced concrete response to simulated earthquakes”, *J. Struct. Div.*, **96**, 2557 - 2573.
- Wolf, J.P. (1985), *Dynamic Soil-Structure Interaction*, Prentice-Hall.
- Wolf, J.P. (1994), *Foundation Vibration Analysis Using Simple Physical Models*, Prentice-Hall.